

AEROELASTIC ANALYSIS OF BRIDGES UNDER MULTICORRELATED WINDS: INTEGRATED STATE-SPACE APPROACH

By Xinzhong Chen¹ and Ahsan Kareem²

ABSTRACT: In this paper, an integrated state-space model of a system with a vector-valued white noise input is presented to describe the dynamic response of bridges under the action of multicorrelated winds. Such a unified model has not been developed before due to a number of innate modeling difficulties. The integrated state-space model is realized based on the state-space models of multicorrelated wind fluctuations, unsteady buffeting and self-excited aerodynamic forces, and the bridge dynamics. Both the equations of motion at the full order in the physical coordinates and at the reduced-order in the generalized modal coordinates are presented. This state-space model allows direct evaluation of the covariance matrix of the response using the Lyapunov equation, which presents higher computational efficiency than the conventional spectral analysis approach. This state-space model also adds time domain simulation of multicorrelated wind fluctuations, the associated unsteady frequency dependent aerodynamic forces, and the attendant motions of the structure. The structural and aerodynamic coupling effects among structural modes can be easily included in the analysis. The model also facilitates consideration of various nonlinearities of both structural and aerodynamic origins in the response analysis. An application of this approach to a long-span cable-stayed bridge illustrates the effectiveness of this scheme for a linear problem. An extension of the proposed analysis framework to include structural and aerodynamic nonlinearities is immediate once the nonlinear structural and aerodynamic characteristics of the bridge are established.

INTRODUCTION

Aerodynamic forces on bridges have conventionally been modeled as the sum of motion-induced self-excited and wind-induced buffeting force components. These are in general functions of the geometric configurations of bridge sections, the incoming wind fluctuations, and the reduced frequency. In the wind velocity range of interest in structural design, the flow around bluff bridge sections is quite unsteady and not amenable to quasi-steady analysis techniques, which are only valid at very high wind velocities. The frequency dependent characteristics of aerodynamic forces are generally described in terms of experimentally quantified flutter derivatives for the self-excited forces and in terms of admittance and spanwise coherence functions for the buffeting forces. Incorporating these unsteady aerodynamic characteristics is essential for an accurate evaluation of the forces and the attendant response of the structures. These characteristics can be easily incorporated in the frequency domain analysis framework with and without the consideration of intermode coupling effects (Davenport 1962; Scanlan 1978a,b; Jain et al. 1996; Katsuchi et al. 1999; Chen et al. 2000a).

To account for the structural and aerodynamic nonlinearities in the analysis, the equations of motion must be cast in the time domain and solved using a time domain scheme. Most previous time domain studies concerning bridge buffeting response have used quasi-steady assumption when modeling the aerodynamic forces. These assumptions manifest themselves by neglecting the frequency dependent flutter derivatives, admittance functions, and effects of spanwise correlation. This inconsistency with the frequency domain approach has been addressed by Chen et al. (2000b), in which the frequency dependent unsteady aerodynamic forces are accurately modeled in the time domain analysis framework. This time domain

approach is regarded as a rigorous representation of the frequency domain analysis of linear problems as long as the aerodynamic forces are represented by rational function approximations (RFAs) exactly or with an acceptable level of error. Recent developments presented in this paper may be viewed as an extension of this time domain approach by utilizing a state-space modeling technique that is rooted in linear system theory.

Much research has been performed in the area of linear state-space modeling of unsteady self-excited aerodynamic forces in the aeronautical field by using RFA technique (e.g., Roger 1977; Karpel 1982). Among these schemes, Roger's RFA is the most widely utilized because of the accuracy, simplicity, and robustness of the method, although different forms of the approximation, such as the minimum state (MS) method, are available with a focus on reducing the dimensions of the augmented aerodynamic states (Karpel 1982). The application of RFAs to bluff body bridge aerodynamics can be found in the representation of the self-excited forces (Scanlan et al. 1974; Lin and Yang 1983; Xie et al. 1985; Bucher and Lin 1988; Matsumoto et al. 1994; Wilde et al. 1996; Boonyapinyo et al. 1999; Chen et al. 2000a,b). The modeling of frequency dependent buffeting forces is given in Matsumoto and Chen (1996), Matsumoto et al. (1996), and Chen et al. (2000b).

The modeling of multicorrelated wind fluctuations in a state-space framework has also been addressed in Goßmann and Walter (1982), Suhardjo et al. (1992), Matsumoto et al. (1996), and Kareem (1997). This is based on factorization of the cross-power spectral density (XPSD) matrix of the wind fluctuations. The spectral matrix is first expressed in terms of RFAs and is then decomposed into a transfer function, which is then utilized to obtain the state-space matrices based on the realization of the transfer function. The modeling of a matrix transfer function and subsequent operations are nontrivial for a large size wind field simulation. In some cases, the mathematical difficulty and numerical error introduced by the calculation procedure precluded the use of this technique to realistic problems (Matsumoto et al. 1996). Kareem (1997) has suggested some simplifications, but the approach remains tedious as attested by a lack of realistic feed-forward modeling of wind in the literature. In Kareem and Mei (1999) and Benfratello and Muscolino (1999), the stochastic decomposition technique is utilized to decompose a multicorrelated random

¹Postdoct. Res. Assoc., Dept. of Civ. Engrg. and Geological Sci., Univ. of Notre Dame, Notre Dame, IN 46556.

²Robert M. Moran Prof. and Chair, Dept. of Civ. Engrg. and Geological Sci., Univ. of Notre Dame, Notre Dame, IN 46556.

Note. Associate Editor: George Deodatis. Discussion open until April 1, 2002. To extend the closing date one month, a written request must be filed with the ASCE Manager of Journals. The manuscript for this paper was submitted for review and possible publication on June 6, 2000; revised April 24, 2001. This paper is part of the *Journal of Engineering Mechanics*, Vol. 127, No. 11, November, 2001. ©ASCE, ISSN 0733-9399/01/0011-1124-1134/\$8.00 + \$.50 per page. Paper No. 22359.

process into a set of independent random subprocesses. For each subprocess the state-space model is derived, and then through a transformation the state-space model of the original multicorrelated process is composed. For simplification of the state-space modeling in the original coordinate space, an eigenvector matrix value at a fixed frequency is chosen based on the observation that the eigenvectors of the XPSD matrix change very slowly with respect to the frequency. This technique requires the eigenvalue analysis of the XPSD matrix at each discrete frequency, which may result in large computational efforts for a large size wind-field simulation. In addition, the assumption of constant eigenvectors may introduce errors in some cases depending on the spectral matrix of wind fluctuations. Chen and Kareem (2000) pointed out that, with the truncation of higher modes of wind fluctuations, this stochastic decomposition technique provides an efficient tool for state-space modeling of well-correlated random processes. Its effectiveness in modeling poorly correlated random processes is rather limited, particularly, for representing high-frequency wind fluctuations.

In this paper, an integrated state-space model of a multiinput and multioutput system with a vector-valued white noise input is presented to model the dynamic response of bridges under the multicorrelated winds. Such a unified model has not been developed before due to a number of innate modeling difficulties. This integrated state-space model is realized based on the state-space models of the multicorrelated wind fluctuations, the unsteady aerodynamic forces, and the structure. Both the equations of motion at the full order in the physical coordinates and at reduced order in the generalized modal coordinates are presented. The full-order form is more appropriate for nonlinear problems by using time-variant system models, whereas the reduced form is computationally more efficient for the linear problems. An application of this approach to a long span cable-stayed bridge demonstrates its effectiveness.

STATE-SPACE REPRESENTATION OF RESPONSE UNDER WINDS

The mathematical model for describing the response of wind-excited structure based on linear system theory is schematically shown in Fig. 1. The wind-induced motions of the structure can be represented as the outputs of an integrated multiinput and multioutput system excited by a vector-valued white noise process. The multicorrelated wind fluctuations are considered as the output of a system with a vector-valued white noise excitation, whose transfer functions can be derived by factorizing their power spectral density matrix. Similarly,

the buffeting forces are derived as the output of a system with wind fluctuations as input. Their transfer functions are described in terms of the admittance function and spanwise coherence of unsteady buffeting forces. Similarly, the self-excited forces are modeled as the output of a system with the structural response as input. Their transfer functions are defined in terms of the flutter derivatives. By augmenting the state-space equations of structural motion with the corresponding state-space representation of the loading components and wind fluctuations, as stated above, an integrated state-space model is established that synthesizes the unsteady characteristics of multicorrelated wind field, frequency dependent unsteady aerodynamic forces, and the dynamics of the bridge.

The integrated state-space model for describing the response of a structure under winds has several significant mathematical advantages. The recasting of the overall system equations in the state-space format allows the use of tools based on linear system theory for response analysis, optimization, and design of active control devices to suppress flutter and buffeting. By using this model, the wind load information can be incorporated in a structural control design as a feed-forward link with the potential to enhance the control effectiveness (Suhardjo et al. 1992). In addition, the structural and aerodynamic coupling effects can be automatically included in the computation. For linear problems, conventional spectral analysis approach requires intensive computational efforts in the estimation of the transfer function and response spectral density matrix at each discrete frequency with an interval that must be very small for bridges with closely spaced natural frequencies. Subsequent integration of the spectral matrix needed to determine the response covariance requires additional computational effort. An integrated linear time-invariant state-space model of the response with a vector-valued white noise input facilitates direct estimation of the covariance matrix of the response through the Lyapunov equation and allows higher computational efficiency.

MODELING OF MULTICORRELATED WINDS

Consider a structure represented by a finite-element discretization. The longitudinal and vertical components of wind fluctuations at the centers of elements, $W(t)$, are represented by a multicorrelated random process. These can be represented as the output of a linear system with input of a vector-valued Gaussian white noise process $N(t)$ with a zero mean and identity covariance matrix. In this study, an autoregressive (AR) model is used to describe this linear system for accurate modeling and simplicity. The AR model is considered as a special

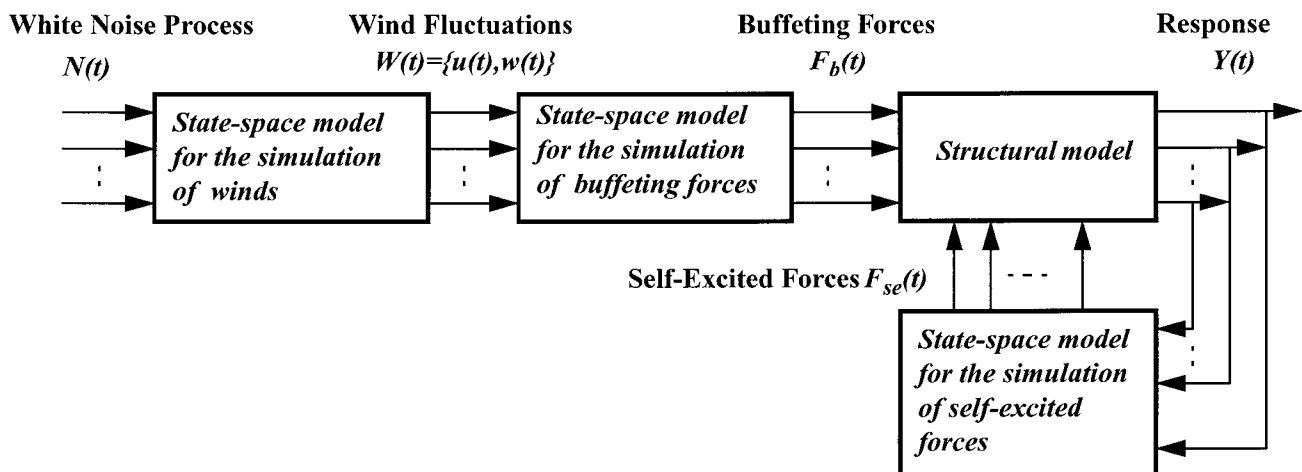


FIG. 1. Integrated Modeling of Dynamic Response of Wind-Excited Structure

case of a general autoregressive moving-average (ARMA) model (e.g., Samaras et al. 1985; Mignolet and Spanos 1987; Li and Kareem 1990a,b).

The AR model is expressed as

$$\mathbf{W}(t) = \sum_{k=1}^p \mathbf{P}_k \mathbf{W}(t - k\Delta t) + \mathbf{L}\mathbf{N}(t) \quad (1)$$

where Δt = time interval; p = model order; and \mathbf{P}_k ($k = 1, 2, \dots, p$) = coefficient matrices satisfying the following Yule-Walker equations:

$$\mathbf{R}_w(j\Delta t) = \sum_{k=1}^p \mathbf{R}_w((j-k)\Delta t) \mathbf{P}_k^T \quad (j = 1, 2, \dots, p) \quad (2)$$

where $\mathbf{R}_w(j\Delta t)$ ($j = 1, 2, \dots, p$) = correlation matrix of the wind fluctuation vector $\mathbf{W}(t)$. In this study, instead of directly using (2), an iterative procedure is utilized to determine the coefficient matrices for enhancing the computational efficiency (Ianuzzi and Spinelli 1987).

The correlation matrix $\mathbf{R}_w(j\Delta t)$ can be evaluated from the spectral density matrix $\mathbf{S}_w(f)$ using the Wiener-Khinchine relationship:

$$\mathbf{R}_w(j\Delta t) = 2 \int_0^{\infty} \mathbf{S}_w(f) \cos(j2\pi f\Delta t) df \quad (3)$$

and the matrix \mathbf{L} is given by the Cholesky factorization:

$$\mathbf{L}^T \mathbf{L} = \mathbf{R}_0 \quad (4)$$

$$\mathbf{R}_0 = \mathbf{R}_w(0) - \sum_{k=1}^p \mathbf{P}_k \mathbf{R}_w(k\Delta t) \quad (5)$$

Once the AR model is developed, there are several ways to express it in terms of a discrete-time state-space format; for example, the controllable canonical form, observable canonical form, diagonal canonical form, and Jordan canonical form (Ogata 1994). In this study, the following controllable canonical form is used:

$$\mathbf{X}_w(t) = \mathbf{A}_{dw} \mathbf{X}_w(t - \Delta t) + \mathbf{B}_{dw} \mathbf{N}(t) \quad (6)$$

$$\mathbf{W}(t) = \mathbf{C}_{dw} \mathbf{X}_w(t) + \mathbf{D}_{dw} \mathbf{N}(t) \quad (7)$$

where

$$\mathbf{X}_w(t) = \begin{bmatrix} \mathbf{X}_{w1}(t) \\ \mathbf{X}_{w2}(t) \\ \vdots \\ \mathbf{X}_{w(p-1)}(t) \\ \mathbf{X}_{wp}(t) \end{bmatrix}; \quad \mathbf{A}_{dw} = \begin{bmatrix} \mathbf{0} & \mathbf{I} & \mathbf{0} & \cdots & \mathbf{0} \\ \mathbf{0} & \mathbf{0} & \mathbf{I} & \cdots & \mathbf{0} \\ \vdots & \vdots & \vdots & \cdots & \vdots \\ \mathbf{0} & \mathbf{0} & \mathbf{0} & \cdots & \mathbf{I} \\ \mathbf{P}_p & \mathbf{P}_{p-1} & \mathbf{P}_{p-2} & \cdots & \mathbf{P}_1 \end{bmatrix} \quad (8a,b)$$

$$\mathbf{B}_{dw} = \begin{bmatrix} \mathbf{0} \\ \mathbf{0} \\ \vdots \\ \mathbf{0} \\ \mathbf{I} \end{bmatrix}; \quad \mathbf{C}_{dw} = [\mathbf{P}_p \mathbf{L} \quad \mathbf{P}_{p-1} \mathbf{L} \quad \cdots \quad \mathbf{P}_1 \mathbf{L}] \quad (8c,d)$$

$$\mathbf{D}_{dw} = \mathbf{L} \quad (8e)$$

The equivalent continuous state-space representation can be given as

$$\dot{\mathbf{X}}_w = \mathbf{A}_w \mathbf{X}_w + \mathbf{B}_w \mathbf{N} \quad (9)$$

$$\mathbf{W} = \mathbf{C}_w \mathbf{X}_w + \mathbf{D}_w \mathbf{N} \quad (10)$$

with the relationship

$$\mathbf{A}_{dw} = e^{\mathbf{A}_w \Delta t}; \quad \mathbf{B}_{dw} = (e^{\mathbf{A}_w \Delta t} - \mathbf{I}) \mathbf{A}_w^{-1} \mathbf{B}_w \quad (11a,b)$$

$$\mathbf{C}_{dw} = \mathbf{C}_w; \quad \mathbf{D}_{dw} = \mathbf{D}_w \quad (11c,d)$$

Similarly, the state-space modeling of a multicorrelated wind field based on a multivariate ARMA model can also be presented, but is omitted here for the sake of brevity. Using such a parametric approach for describing random processes not only facilitates efficient simulation, but it also provides an efficient and robust tool for the state-space modeling of random processes compared with alternative approaches alluded to earlier.

MODELING OF UNSTEADY BUFFETING FORCES

The buffeting force components per unit length, i.e., lift (downward), drag (downwind), and pitching moment (nose-up), induced by a sinusoidal wind fluctuation with circular frequency ω , are commonly expressed (e.g., Scanlan 1978a,b; Chen et al. 2000a,b) as

$$L_b(t) = -\frac{1}{2} \rho U^2 B \left(2C_L \chi_{L_{bu}}(ik) \frac{u(t)}{U} + (C'_L + C_D) \chi_{L_{bw}}(ik) \frac{w(t)}{U} \right) \quad (12)$$

$$D_b(t) = \frac{1}{2} \rho U^2 B \left(2C_D \chi_{D_{bu}}(ik) \frac{u(t)}{U} + (C'_D - C_L) \chi_{D_{bw}}(ik) \frac{w(t)}{U} \right) \quad (13)$$

$$M_b(t) = \frac{1}{2} \rho U^2 B^2 \left(2C_M \chi_{M_{bu}}(ik) \frac{u(t)}{U} + C'_M \chi_{M_{bw}}(ik) \frac{w(t)}{U} \right) \quad (14)$$

where ρ = air density; U = mean wind velocity; $B = 2b$ is the bridge deck width; C_D , C_L , C_M = static force coefficients; $C'_L = dC_L/d\alpha$ and $C'_M = dC_M/d\alpha$; u and w = longitudinal and vertical wind fluctuations, respectively; $\chi_r(ik)$ ($r = L_{bu}$, L_{bw} , D_{bu} , D_{bw} , M_{bu} , M_{bw}) denote the aerodynamic transfer functions between wind fluctuations and buffeting forces per unit span, and their absolute magnitudes are referred to as the aerodynamic admittance functions; $k = \omega b/U$ is the reduced frequency; and i = pure imaginary unit $\sqrt{-1}$.

Accordingly, the buffeting forces acting on a beam element of length l can be given by

$$\mathbf{F}_b^e(t) = (\rho U^2 B l) \mathbf{A}_b^e(ik) \mathbf{W}^e \quad (15)$$

where

$$\mathbf{A}_b^e = \begin{bmatrix} C_{L1} \chi_{L_{bu}}(ik) J_{L_{bu}}(ik) & C_{L2} \chi_{L_{bw}}(ik) J_{L_{bw}}(ik) \\ C_{D1} \chi_{D_{bu}}(ik) J_{D_{bu}}(ik) & C_{D2} \chi_{D_{bw}}(ik) J_{D_{bw}}(ik) \\ BC_{M1} \chi_{M_{bu}}(ik) J_{M_{bu}}(ik) & BC_{M2} \chi_{M_{bw}}(ik) J_{M_{bw}}(ik) \end{bmatrix} \quad (16a)$$

$$\mathbf{F}_b^e = [L_b^e \quad D_b^e \quad M_b^e]^T; \quad \mathbf{W}^e = [u^e/U \quad w^e/U]^T \quad (16b,c)$$

$$C_{L1} = -C_L; \quad C_{L2} = -\frac{1}{2} (C'_L + C_D); \quad C_{D1} = C_D \quad (16d-f)$$

$$C_{D2} = \frac{1}{2} (C'_D - C_L); \quad C_{M1} = C_M; \quad C_{M2} = \frac{1}{2} C'_M \quad (16g-i)$$

u^e and w^e = wind fluctuations at the center of the element; superscript e indicates the component on the element; superscript T indicates matrix transpose; and $J_r(ik)$ ($r = L_{bu}$, L_{bw} , D_{bu} , D_{bw} , M_{bu} , M_{bw}) denotes the joint acceptance functions that describe the reduction effect of the buffeting forces due to the loss of spanwise correlation within the element, as compared with the fully correlated case, and expressed as

$$|J_r|^2 = \frac{1}{l^2} \int_0^l \int_0^l \text{coh}_r(x_1, x_2; f) dx_1 dx_2 \quad (17)$$

where $\text{coh}_r(x_1, x_2; f)$ = coherence fluctuation of buffeting forces; and x_1 and x_2 = coordinates of points 1 and 2 in the

across-wind direction. For tower and cable elements of cable-supported bridges, only the drag component is generally considered in the analysis of overall bridge response.

The state-space modeling of F_b^e will be accomplished in two steps. The first step is to model the admittance function $\chi_r(ik)$, and the second step is to model the joint acceptance function $J_r(ik)$. These are expressed as the following rational function approximations (Chen et al. 2000b), although other forms can also be utilized:

$$\chi_r(ik) = A_{r,1}^x + \sum_{j=1}^{m_x'} \frac{(ik)A_{r,j+1}^x}{ik + d_{r,j}^x} \quad (18)$$

$$J_r(ik) = A_{r,1}^j + \sum_{j=1}^{m_j'} \frac{(ik)A_{r,j+1}^j}{ik + d_{r,j}^j} \quad (19)$$

Accordingly, the state-space equations for F_b^e are then written (Appendix I) as

$$\dot{\mathbf{X}}_b^e = \mathbf{A}_b^e \mathbf{X}_b^e + \mathbf{B}_b^e \mathbf{W}^e \quad (20)$$

$$\mathbf{F}_b^e = \mathbf{C}_b^e \mathbf{X}_b^e + \mathbf{D}_b^e \mathbf{W}^e \quad (21)$$

Based on the finite-element procedure, for an assumed shape function of displacement within an element, the nodal forces in the local coordinate system can be expressed using the state-space model. Subsequently, the total nodal buffeting forces for the entire structure can be obtained by transforming the nodal forces in the local coordinates to the global coordinate system and assembling the element forces. The total nodal force $\mathbf{F}_b(t)$ can be finally expressed in terms of state-space equations with the input of wind fluctuations, $\mathbf{W}(t)$, as

$$\dot{\mathbf{X}}_b = \mathbf{A}_b \mathbf{X}_b + \mathbf{B}_b \mathbf{W} \quad (22)$$

$$\mathbf{F}_b = \mathbf{C}_b \mathbf{X}_b + \mathbf{D}_b \mathbf{W} \quad (23)$$

When the buffeting forces are simply expressed using the quasi-steady theory, i.e., $\chi_r = J_r = 1$, the state-space model of buffeting forces then becomes

$$\mathbf{F}_b^e = \mathbf{D}_{bqs}^e \mathbf{W}^e \quad (24)$$

where

$$\mathbf{D}_{bqs}^e = (\rho U^2 B l) \begin{bmatrix} C_{L1} & C_{L2} \\ C_{D1} & C_{D2} \\ BC_{M1} & BC_{M2} \end{bmatrix} \quad (25)$$

Accordingly, \mathbf{F}_b is expressed as

$$\mathbf{F}_b = \mathbf{D}_{bqs} \mathbf{W} \quad (26)$$

Clearly, the quasi-steady description of buffeting forces eliminates the augmented states representing the unsteady properties of the buffeting forces. Therefore, the current state-space model more accurately represents the frequency dependent unsteady characteristics of the aerodynamic forces, which are essential for the response analysis in both time and frequency domains.

An alternative approach for the state-space modeling of buffeting forces is directly based on their XPSD matrix and subsequently expressed in terms of an AR model, similar to the case of multicorrelated wind fluctuations. However, the approach presented here is more consistent when considering aerodynamic nonlinearities, such as the dependency of aerodynamic parameters on the effective angle of wind incidence. In this case, wind fluctuations must be simulated to accommodate the consideration of the nonlinear effects.

It is worth noting that the spanwise correlation of the buffeting forces is generally higher than that of the incoming wind fluctuations (e.g., Kareem 1990; Larose and Mann 1998). To

accurately describe the spanwise correlation of buffeting forces, the spatial properties of buffeting forces—and not those of the incident wind—may be used in the evaluation of the spectral matrix of the wind fluctuations modeled in the above section. This correction to the model of wind fluctuations generates what is referred to as the “effective” wind fluctuations rather than a realization of the original wind field. In this study, this correction of spatial correlation of wind fluctuations is used to model the more complex generation mechanism of buffeting forces, which is currently mathematically intractable.

The cospectrum between the wind fluctuations on the centers of i th and j th elements are given as

$$S_{r_{ij}}(f) = \text{coh}_{ij}(f) \sqrt{S_{r_i}(f) S_{r_j}(f)} \quad (r = u, w) \quad (27)$$

$$\text{coh}_{ij}(f) = \frac{1}{l_i l_j} \int_0^{l_i} \int_0^{l_j} \text{coh}_r(x_1, x_2; f) dx_1 dx_2 (|J_{r_i}||J_{r_j}|) \quad (28)$$

where l_i and l_j = lengths of i th and j th elements, respectively; and J_{r_i} and J_{r_j} = joint acceptance functions of the i th and j th elements [(17)].

MODELING OF SELF-EXCITED FORCES

The self-excited force components per unit length induced by a sinusoidal motion with circular frequency ω are expressed in terms of flutter derivatives H_i^* , P_i^* , and A_i^* ($i = 1, 2, \dots, 6$) (e.g., Scanlan 1978a,b; Jain et al. 1996; Katsuchi et al. 1999; Chen et al. 2000a,b) as

$$L_{se}(t) = \frac{1}{2} \rho U^2 (2b) \left(kH_1^* \frac{\dot{h}}{U} + kH_2^* \frac{b\dot{\alpha}}{U} + k^2 H_3^* \alpha + k^2 H_4^* \frac{h}{b} + kH_5^* \frac{\dot{p}}{U} + k^2 H_6^* \frac{p}{b} \right) \quad (29)$$

$$D_{se}(t) = \frac{1}{2} \rho U^2 (2b) \left(kP_1^* \frac{\dot{p}}{U} + kP_2^* \frac{b\dot{\alpha}}{U} + k^2 P_3^* \alpha + k^2 P_4^* \frac{p}{b} + kP_5^* \frac{\dot{h}}{U} + k^2 P_6^* \frac{h}{b} \right) \quad (30)$$

$$M_{se}(t) = \frac{1}{2} \rho U^2 (2b^2) \left(kA_1^* \frac{\dot{h}}{U} + kA_2^* \frac{b\dot{\alpha}}{U} + k^2 A_3^* \alpha + k^2 A_4^* \frac{h}{b} + kA_5^* \frac{\dot{p}}{U} + k^2 A_6^* \frac{p}{b} \right) \quad (31)$$

The self-excited forces are commonly assumed to be fully correlated in spanwise direction. Although a loss of spanwise correlation of the self-excited forces can affect the aerodynamic damping and the flutter stability (Scanlan 1997), a recent experiment study has reported only slight turbulence effects on self-excited force correlation (Haan et al. 1999; Haan 2000). In this study, full correlation of the self-excited forces is assumed. Further experimental investigation of this issue needs to be undertaken. Once a working model for the spanwise correlation of the self-excited forces becomes available, the analysis framework presented here can incorporate it conveniently without further modification.

The self-excited forces acting on a beam element of length l can be given as

$$\mathbf{F}_{se}^e(t) = \frac{1}{2} \rho U^2 \left(\mathbf{A}_s^e(ik) \mathbf{Y}^e(t) + \frac{b}{U} \mathbf{A}_s^e(ik) \dot{\mathbf{Y}}^e(t) \right) \quad (32)$$

where

$$\mathbf{A}_s^e(ik) = \begin{bmatrix} 2k^2lH_4^* & 2k^2lH_6^* & 2k^2lbH_3^* \\ 2k^2lP_6^* & 2k^2lP_4^* & 2k^2lbP_3^* \\ 2k^2blA_4^* & 2k^2blA_6^* & 2k^2b^2lA_3^* \end{bmatrix} \quad (33a)$$

$$\mathbf{A}_d^e(ik) = \begin{bmatrix} 2klH_1^* & 2klH_5^* & 2klbH_2^* \\ 2klP_5^* & 2klP_1^* & 2klbP_2^* \\ 2kblA_1^* & 2kblA_5^* & 2kb^2lA_2^* \end{bmatrix} \quad (33b)$$

$$\mathbf{F}_{se}^e(t) = [L_{se}^e(t) \quad D_{se}^e(t) \quad M_{se}^e(t)]^T \quad (33c)$$

$$\mathbf{Y}^e = [h^e(t) \quad p^e(t) \quad \alpha^e(t)]^T \quad (33d)$$

and h^e , p^e , and α^e = vertical, lateral, and torsional displacement at the center of the element, respectively; and the over-dot denotes the differentiation with respect to time.

The transfer matrix between the self-excited forces and the structural motion can be represented by the following RFA in terms of the reduced frequency k . This is accomplished by fitting the tabular data $\mathbf{H}_{se}^e(ik_j)$ defined at a set of discrete reduced frequencies k_j ($j = 1, 2, \dots$) for which these transfer function matrices are available (Roger 1977; Chen et al. 2000a,b):

$$\mathbf{H}_{se}^e(ik) = \mathbf{A}_s^e + (ik)\mathbf{A}_d^e = \mathbf{A}_1^e + (ik)\mathbf{A}_2^e + (ik)^2\mathbf{A}_3^e + \sum_{j=1}^{m^e} \frac{(ik)\mathbf{A}_{j+3}^e}{ik + d_j^e} \quad (34)$$

where \mathbf{A}_1^e , \mathbf{A}_2^e , \mathbf{A}_3^e , \mathbf{A}_{j+3}^e , and d_j^e ($d_j^e \geq 0$; $j = 1, 2, \dots, m^e$) = frequency independent matrices and parameters; and m^e is the order of RFA.

Replacing the Fourier transform by a Laplace transform through analytic continuation with \bar{s} [where $\bar{s} = (-\xi + i)k$, and ξ = damping ratio of the motion) substituted for ik , and by taking an inverse Laplace transform, the self-excited forces induced by an arbitrary motion can be expressed in terms of the following state-space equations:

$$\dot{\mathbf{X}}_{sej}^e(t) = -\frac{d_j^e U}{b} \mathbf{X}_{sej}^e(t) + \mathbf{A}_{j+3}^e \dot{\mathbf{Y}}^e(t) \quad (j = 1, 2, \dots, m^e) \quad (35)$$

$$\mathbf{F}_{se}^e(t) = \frac{1}{2} \rho U^2 \left(\mathbf{A}_1^e \mathbf{Y}^e(t) + \frac{b}{U} \mathbf{A}_2^e \dot{\mathbf{Y}}^e(t) + \frac{b^2}{U^2} \mathbf{A}_3^e \ddot{\mathbf{Y}}^e(t) + \sum_{j=1}^{m^e} \mathbf{X}_{sej}^e(t) \right) \quad (36)$$

where \mathbf{X}_{sej}^e ($j = 1, 2, \dots, m^e$) = augmented new variables representing the aerodynamic states.

Based on the finite-element procedure, the total self-excited forces can be finally expressed in terms of the nodal motion \mathbf{Y} as

$$\dot{\mathbf{X}}_{sej}^e(t) = -\frac{d_j U}{b} \mathbf{X}_{sej}^e(t) + \mathbf{A}_{j+3} \dot{\mathbf{Y}}(t) \quad (j = 1, 2, \dots, m) \quad (37)$$

$$\mathbf{F}_{se}(t) = \frac{1}{2} \rho U^2 \left(\mathbf{A}_1 \mathbf{Y}(t) + \frac{b}{U} \mathbf{A}_2 \dot{\mathbf{Y}}(t) + \frac{b^2}{U^2} \mathbf{A}_3 \ddot{\mathbf{Y}}(t) + \sum_{j=1}^m \mathbf{X}_{sej}(t) \right) \quad (38)$$

where \mathbf{A}_1 , \mathbf{A}_2 , \mathbf{A}_3 , \mathbf{A}_{j+3} , and d_j ($d_j \geq 0$; $j = 1, 2, \dots, m$) = frequency independent matrices and parameters; m is the order of RFA; and $\mathbf{X}_{sej}(t)$ ($j = 1, 2, \dots, m$) = augmented aerodynamic states.

It is worth mentioning that, when the self-excited forces are modeled using the quasi-steady theory, only matrices \mathbf{A}_1 and \mathbf{A}_2 are included in the model, thus eliminating the augmented aerodynamic states \mathbf{X}_{sej} ($j = 1, 2, \dots, m$).

FULL-ORDER INTEGRATED STATE-SPACE MODEL

The governing equations of motion with respect to the static equilibrium position of a bridge are given in matrix form by

$$\mathbf{M}\ddot{\mathbf{Y}} + \mathbf{C}\dot{\mathbf{Y}} + \mathbf{K}\mathbf{Y} = \mathbf{F}_{se} + \mathbf{F}_b \quad (39)$$

where \mathbf{M} , \mathbf{C} , and \mathbf{K} = mass, damping, and stiffness matrices, respectively.

Substituting (9), (10), (22), (23), (37), and (38) into the above equation, the following state-space equations are obtained:

$$\dot{\mathbf{X}} = \mathbf{A}\mathbf{X} + \mathbf{B}\mathbf{N} \quad (40)$$

$$\mathbf{Y} = \mathbf{G}\mathbf{X} \quad (41)$$

where

$$\mathbf{X} = \begin{bmatrix} \mathbf{X}_{sse} \\ \mathbf{X}_b \\ \mathbf{X}_w \end{bmatrix}; \quad \mathbf{A} = \begin{bmatrix} \mathbf{A}_{sse} & \mathbf{B}_{sse}\mathbf{C}_b & \mathbf{B}_{sse}\mathbf{D}_b\mathbf{C}_w \\ \mathbf{0} & \mathbf{A}_b & \mathbf{B}_b\mathbf{C}_w \\ \mathbf{0} & \mathbf{0} & \mathbf{A}_w \end{bmatrix} \quad (42a,b)$$

$$\mathbf{B} = \begin{bmatrix} \mathbf{B}_{sse}\mathbf{D}_b\mathbf{D}_w \\ \mathbf{B}_b\mathbf{D}_w \\ \mathbf{B}_w \end{bmatrix}; \quad \mathbf{G} = \begin{bmatrix} \mathbf{C}_{sse} \\ \mathbf{0} \\ \mathbf{0} \end{bmatrix}^T \quad (42c,d)$$

$$\mathbf{X}_{sse} = \begin{bmatrix} \mathbf{Y} \\ \dot{\mathbf{Y}} \\ \mathbf{X}_{se1} \\ \vdots \\ \mathbf{X}_{sem} \end{bmatrix} \quad (42e)$$

$$\mathbf{A}_{sse} = \begin{bmatrix} \mathbf{0} & \mathbf{I} & \mathbf{0} & \cdots & \mathbf{0} \\ -\bar{\mathbf{M}}^{-1}\bar{\mathbf{K}} & -\bar{\mathbf{M}}^{-1}\bar{\mathbf{C}} & \frac{1}{2}\rho U^2\bar{\mathbf{M}}^{-1} & \cdots & \frac{1}{2}\rho U^2\bar{\mathbf{M}}^{-1} \\ \mathbf{0} & \mathbf{A}_4 & -\frac{U}{b}d_1\mathbf{I} & \cdots & \mathbf{0} \\ \vdots & \vdots & \vdots & \ddots & \vdots \\ \mathbf{0} & \mathbf{A}_{3+m} & \mathbf{0} & \cdots & -\frac{U}{b}d_m\mathbf{I} \end{bmatrix} \quad (42f)$$

$$\mathbf{B}_{sse} = [\mathbf{0} \quad \bar{\mathbf{M}}^{-1} \quad \mathbf{0} \quad \cdots \quad \mathbf{0}]^T \quad (42g)$$

$$\mathbf{C}_{sse} = [\mathbf{I} \quad \mathbf{0} \quad \mathbf{0} \quad \cdots \quad \mathbf{0}]^T \quad (42h)$$

$$\bar{\mathbf{M}} = \mathbf{M} - \frac{1}{2}\rho b^2\mathbf{A}_3; \quad \bar{\mathbf{C}} = \mathbf{C} - \frac{1}{2}\rho U b \mathbf{A}_2 \quad (42i,j)$$

$$\bar{\mathbf{K}} = \mathbf{K} - \frac{1}{2}\rho U^2\mathbf{A}_3 \quad (42k)$$

The solution of above equation can be obtained (Soong and Grigoriu 1993) by

$$\mathbf{X}(t) = e^{\mathbf{A}(t-t_0)}\mathbf{X}(t_0) + \int_{t_0}^t e^{\mathbf{A}(t-\tau)}\mathbf{B}\mathbf{N}(\tau) d\tau \quad (43)$$

The previous equation in a discrete form is given by

$$\mathbf{X}(t) = e^{\mathbf{A}\Delta t}\mathbf{X}(t - \Delta t) + (e^{\mathbf{A}\Delta t} - \mathbf{I})\mathbf{A}^{-1}\mathbf{B}\mathbf{N}(t) \quad (44)$$

where Δt = time interval.

The covariance matrix \mathbf{R}_x can be directly calculated by solving the following Lyapunov equation:

$$\dot{\mathbf{R}}_x = \mathbf{A}\mathbf{R}_x + \mathbf{R}_x\mathbf{A}^T + \mathbf{B}\mathbf{B}^T \quad (45)$$

For the time-invariant case, it reduces to

$$\mathbf{A}\mathbf{R}_x + \mathbf{R}_x\mathbf{A}^T + \mathbf{B}\mathbf{B}^T = 0 \quad (46)$$

REDUCED-ORDER STATE-SPACE MODEL

For linear structures, reduced-order equations of motion in terms of the generalized modal coordinates \mathbf{q} can be utilized for computational convenience:

$$\mathbf{M}_0\ddot{\mathbf{q}} + \mathbf{C}_0\dot{\mathbf{q}} + \mathbf{K}_0\mathbf{q} = \mathbf{Q}_{se} + \mathbf{Q}_b \quad (47)$$

where $\mathbf{M}_0 = \Psi^T\mathbf{M}\Psi$, $\mathbf{C}_0 = \Psi^T\mathbf{C}\Psi$, and $\mathbf{K}_0 = \Psi^T\mathbf{K}\Psi =$ generalized mass, damping, and stiffness matrices, respectively; $\mathbf{Q}_{se} = \Psi^T\mathbf{F}_{se}$ and $\mathbf{Q}_b = \Psi^T\mathbf{F}_b$ are the generalized self-excited and buffeting force vectors, respectively; and $\Psi =$ mode shape matrix.

The state-space equations of \mathbf{Q}_b can be given as follows based on the state-space model of \mathbf{F}_b [(22) and (23)]:

$$\dot{\mathbf{X}}_b = \mathbf{A}_b\mathbf{X}_b + \mathbf{B}_b\mathbf{W} \quad (48)$$

$$\mathbf{Q}_b = \mathbf{C}_{b0}\mathbf{X}_b + \mathbf{D}_{b0}\mathbf{W} \quad (49)$$

where $\mathbf{C}_{b0} = \Psi^T\mathbf{C}_b$, $\mathbf{D}_{b0} = \Psi^T\mathbf{D}_b$.

The state-space equations of \mathbf{Q}_{se} can be given as follows based on the state-space model of \mathbf{F}_{se} [(37) and (38)]:

$$\dot{\mathbf{q}}_{sej}(t) = -\frac{d_j U}{b} \mathbf{q}_{sej}(t) + \mathbf{Q}_{j+3} \dot{\mathbf{q}}(t) \quad (j = 1, 2, \dots, m) \quad (50)$$

$$\mathbf{Q}_{se}(t) = \frac{1}{2} \rho U^2 \left(\mathbf{Q}_1 \mathbf{q}(t) + \frac{b}{U} \mathbf{Q}_2 \dot{\mathbf{q}}(t) + \frac{b^2}{U^2} \mathbf{Q}_3 \ddot{\mathbf{q}}(t) + \sum_{j=1}^m \mathbf{q}_{sej}(t) \right) \quad (51)$$

where $\mathbf{Q}_1 = \Psi^T\mathbf{A}_1\Psi$; $\mathbf{Q}_2 = \Psi^T\mathbf{A}_2\Psi$; $\mathbf{Q}_3 = \Psi^T\mathbf{A}_3\Psi$; $\mathbf{Q}_{j+3} = \Psi^T\mathbf{A}_{j+3}\Psi$; and $\mathbf{q}_{sej}(t) = \Psi^T\mathbf{X}_{sej}(t)$ ($j = 1, 2, \dots, m$).

An alternative approach for modeling the generalized self-excited forces is to directly fit the generalized modal aerodynamic matrices calculated at discrete reduced frequencies. If a smaller number of lag terms can thus be obtained, it will lead to reduced aerodynamic states.

Accordingly, the integrated state-space model of the system is given by

$$\dot{\mathbf{X}}_0 = \mathbf{A}_0\mathbf{X}_0 + \mathbf{B}_0\mathbf{N} \quad (52)$$

$$\mathbf{Y} = \Psi^T\mathbf{G}_0\mathbf{X}_0 \quad (53)$$

where

$$\mathbf{X}_0 = \begin{bmatrix} \mathbf{X}_{sse0} \\ \mathbf{X}_b \\ \mathbf{X}_w \end{bmatrix}; \quad \mathbf{A}_0 = \begin{bmatrix} \mathbf{A}_{sse0} & \mathbf{B}_{sse0}\mathbf{C}_{b0} & \mathbf{B}_{sse0}\mathbf{D}_{b0}\mathbf{C}_w \\ \mathbf{0} & \mathbf{A}_b & \mathbf{B}_b\mathbf{C}_w \\ \mathbf{0} & \mathbf{0} & \mathbf{A}_w \end{bmatrix} \quad (54a,b)$$

$$\mathbf{B}_0 = \begin{bmatrix} \mathbf{B}_{sse0}\mathbf{D}_{b0}\mathbf{D}_w \\ \mathbf{B}_b\mathbf{D}_w \\ \mathbf{B}_w \end{bmatrix}; \quad \mathbf{G}_0 = \begin{bmatrix} \mathbf{C}_{sse0} \\ \mathbf{0} \\ \mathbf{0} \end{bmatrix}^T \quad (54c,d)$$

$$\mathbf{X}_{sse0} = \begin{bmatrix} \mathbf{q} \\ \dot{\mathbf{q}} \\ \mathbf{q}_{se1} \\ \vdots \\ \mathbf{q}_{sem} \end{bmatrix} \quad (54e)$$

$$\mathbf{A}_{sse0} = \begin{bmatrix} \mathbf{0} & \mathbf{I} & \mathbf{0} & \cdots & \mathbf{0} \\ -\bar{\mathbf{M}}_0^{-1}\bar{\mathbf{K}}_0 & -\bar{\mathbf{M}}_0^{-1}\bar{\mathbf{C}}_0 & \frac{1}{2}\rho U^2\bar{\mathbf{M}}_0^{-1} & \cdots & \frac{1}{2}\rho U^2\bar{\mathbf{M}}_0^{-1} \\ \mathbf{0} & \mathbf{Q}_4 & -\frac{U}{b}d_1\mathbf{I} & \cdots & \mathbf{0} \\ \vdots & \vdots & \vdots & \ddots & \vdots \\ \mathbf{0} & \mathbf{Q}_{3+m} & \mathbf{0} & \cdots & -\frac{U}{b}d_m\mathbf{I} \end{bmatrix} \quad (54f)$$

$$\mathbf{B}_{sse0} = [\mathbf{0} \quad \bar{\mathbf{M}}_0^{-1} \quad \mathbf{0} \quad \dots \quad \mathbf{0}]^T \quad (54g)$$

$$\mathbf{C}_{sse0} = [\mathbf{I} \quad \mathbf{0} \quad \mathbf{0} \quad \dots \quad \mathbf{0}]^T \quad (54h)$$

$$\bar{\mathbf{M}}_0 = \mathbf{M}_0 - \frac{1}{2}\rho b^2\mathbf{Q}_3; \quad \bar{\mathbf{C}}_0 = \mathbf{C}_0 - \frac{1}{2}\rho U b \mathbf{Q}_2 \quad (54i,j)$$

$$\bar{\mathbf{K}}_0 = \mathbf{K}_0 - \frac{1}{2}\rho U^2\mathbf{Q}_3 \quad (54k)$$

When considering a linear aerodynamic problem, the state-space modeling of \mathbf{Q}_b can be further simplified using a multivariate AR model with a vector-valued white noise input \mathbf{N}_1 , which can be derived based on the XPSD matrix of \mathbf{Q}_b . Accordingly, it can be expressed as

$$\dot{\mathbf{X}}_{b1} = \mathbf{A}_{b1}\mathbf{X}_{b1} + \mathbf{B}_{b1}\mathbf{N}_1 \quad (55)$$

$$\mathbf{Q}_b = \mathbf{C}_{b1}\mathbf{X}_{b1} + \mathbf{D}_{b1}\mathbf{N}_1 \quad (56)$$

and the integrated state-space equations of the system are

$$\dot{\mathbf{X}}_1 = \mathbf{A}_1\mathbf{X}_1 + \mathbf{B}_1\mathbf{N}_1 \quad (57)$$

$$\mathbf{Y} = \Psi\mathbf{G}_1\mathbf{X}_1 \quad (58)$$

where

$$\mathbf{X}_1 = \begin{bmatrix} \mathbf{X}_{sse0} \\ \mathbf{X}_{b1} \end{bmatrix}; \quad \mathbf{A}_1 = \begin{bmatrix} \mathbf{A}_{sse0} & \mathbf{B}_{sse0}\mathbf{C}_{b1} \\ \mathbf{0} & \mathbf{A}_{b1} \end{bmatrix} \quad (59a,b)$$

$$\mathbf{B}_1 = \begin{bmatrix} \mathbf{B}_{sse0}\mathbf{D}_{b1} \\ \mathbf{B}_{b1} \end{bmatrix}; \quad \mathbf{G}_1 = \begin{bmatrix} \mathbf{C}_{sse0} \\ \mathbf{0} \end{bmatrix}^T \quad (59c,d)$$

EXAMPLE

In this section an example is presented to illustrate the integrated state-space analysis framework developed in this study. The example bridge is a cable-stayed bridge with a main span of approximately 1,000 m. For simplicity and without loss of generality, only the aerodynamic forces acting on the bridge deck were considered. The von Karman spectra were used for describing the power spectra of the u and w components of wind fluctuations. For u and w components, turbulence intensities and integral length scales equal to 10 and 7.5%, and 80 and 40 m, respectively, were considered. Higher length scales were used in the evaluation of the coherence function of wind fluctuations in order to account for the stronger spanwise correlation in the buffeting forces than those of the wind fluctuations. Length scales were chosen as 160 and 80 m for the buffeting force component associated to the u and w components, respectively, although these can be determined based on wind tunnel tests (e.g., Larose and Mann 1998).

The bridge deck was discretized into 43 elements along the span. In this study, the u and w components were assumed to

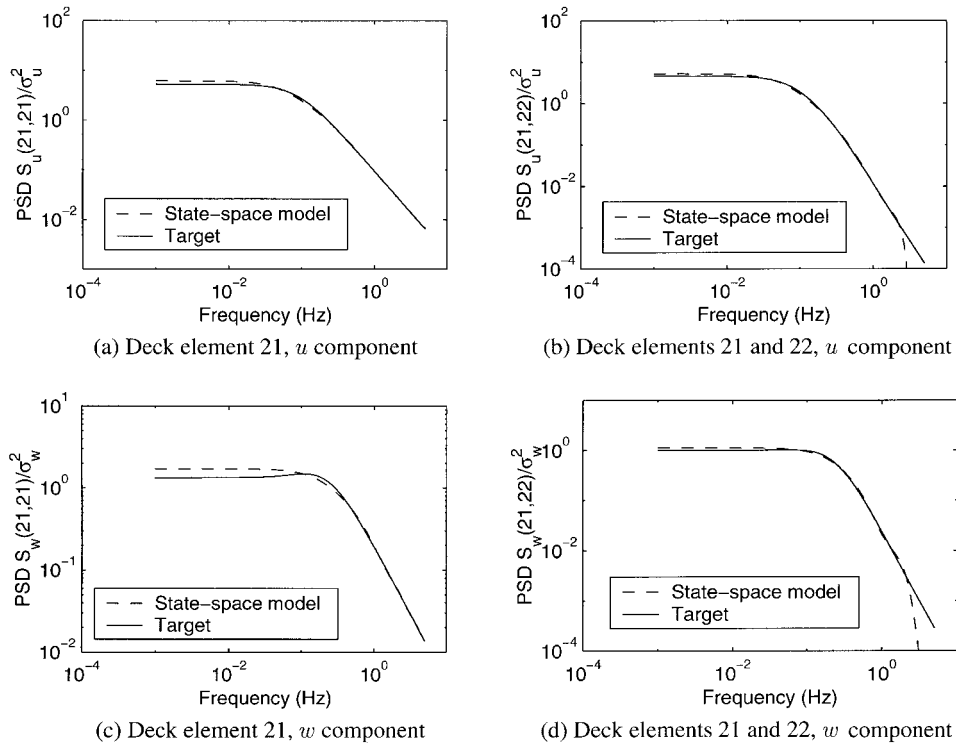


FIG. 2. Comparison of Simulated and Target Auto- and Cross-Power Spectra of Wind Fluctuations ($U = 60$ m/s): (a) Deck Element 21, u Component; (b) Deck Elements 21 and 22, u Component; (c) Deck Element 21, w Component; (d) Deck Elements 21 and 22, w Component

be independent; therefore, these can be expressed using two separate state-space models. The modeling is straightforward for the cases considering the correlation between u and w components of wind fluctuations. Separating wind fluctuations and corresponding buffeting forces and responses into two groups associated to the u and w components will lead to computational efficiency over a combined representation, because computational efforts related to the treatment of cross terms between the u and w components are eliminated. In this example, two state-space models with 258 states each were used for the u and w components of wind fluctuations.

Fig. 2 shows the comparison of the power spectra and cross-spectra of wind fluctuations at elements 21 and 22. The solid and dashed lines are the target and the calculated values from the state-space model, respectively. The results show an excellent agreement, which demonstrates the accuracy of the state-space model.

For each element, different admittance functions for u and w components were used, which were all expressed using RFAs with two rational terms. Davenport's formula with a decay factor of 8 was used for drag, and the Sears function was used for lift and pitching moment. Two different joint acceptance functions were used for buffeting force components associated with u and w components. These were also expressed using RFAs with two rational terms. The dimensions of the state-vector for the buffeting forces acting on each element and the overall structure were 6 and 258, respectively, and were the same for both components corresponding to u and w components of wind fluctuations.

Fig. 3 shows the comparison of the power spectra of the buffeting forces F_b^e acting on element 21. The dashed and solid lines represent the results from the state-space model and the spectral analysis, which is given as follows, based on (15):

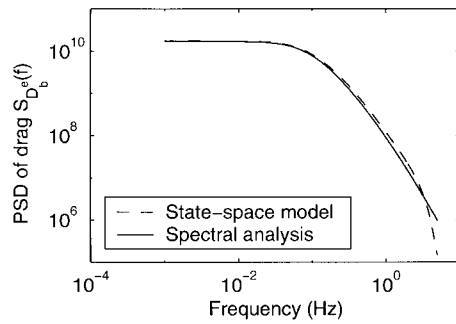
$$\mathbf{S}_{F_b^e}(ik) = (\rho U^2 B l)^2 \mathbf{A}_b^e(ik) \mathbf{S}_w^e \mathbf{A}_b^{eT}(-ik) \quad (60)$$

The drag component of the self-excited forces due to lateral motion was evaluated based on the quasi-steady theory, and

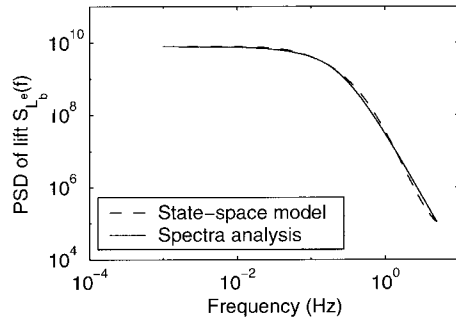
the components relevant to the vertical and torsional motions were neglected. The lift and pitching moment components of the self-excited forces were calculated based on the Theodorsen function. The generalized self-excited forces on the first 12 bridge deck dominated natural modes were expressed using RFA with two rational terms. A reduced-order structural model was used. The natural frequencies range from 0.07 to 0.06 Hz. The logarithmic decrement for each mode was assumed to be 0.02. The total dimension of the state-vectors of the integrated system corresponding to u and w components were both equal to 564. For each of these two integrated systems, the covariance matrix was calculated using the Lyapunov equation to obtain the covariance of the total response.

Fig. 4 shows the comparison of the root mean square (RMS) buffeting response along the span in the vertical, lateral, and torsional directions at mean wind velocities of 40, 60, and 80 m/s. The dashed lines and the dots are the results from the spectral analysis and the present approach, respectively. Results indicate that the state-space model approach gives results that are very close to those from conventional approach, while the state-space model is computationally more efficient. For the example presented here, computational effort using the proposed scheme is less than half of that needed for conventional spectral approach.

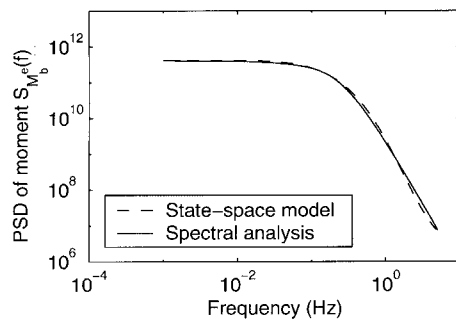
Based on the integrated state-space model, the wind fluctuations, the associated aerodynamic forces, and the buffeting response can be simulated in the time domain by using Monte Carlo simulation. Sample realizations of this simulation are shown in Fig. 5, which represent the u and w components of wind fluctuations at the midpoint of the main span, the drag, lift, and moment components of the buffeting and self-excited forces acting on the beam element at the center of the main span, and the buffeting response in the lateral, vertical, and torsional directions at the midpoint of the main span. It is noted that the buffeting drag force is mainly contributed by the u component of wind fluctuations, while the buffeting lift and pitching moment are mainly contributed by the w com-



(a) Drag component



(b) Lift component



(c) Moment component

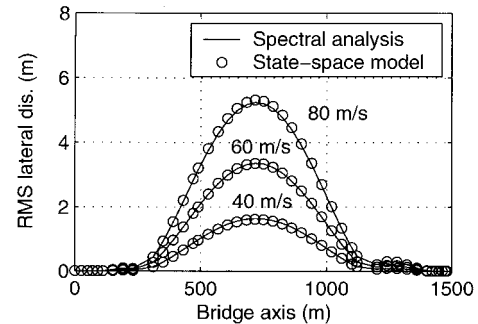
FIG. 3. Comparison of Power Spectra of Buffeting Forces Acting on Deck Element 21 ($U = 60$ m/s): (a) Drag Component; (b) Lift Component; (c) Moment Component

ponent of wind fluctuations. It is also noted that the vertical and torsional response exhibit coupling. The critical flutter velocity was found to be 113.8 m/s utilizing a stability analysis of this integrated system through the solution of the complex eigenvalue problem.

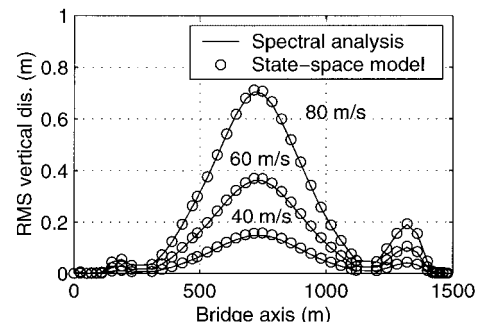
CONCLUDING REMARKS

An integrated state-space model of a multiinput and multioutput system with a vector-valued white noise input was presented to describe the dynamic response of bridges under multicorrelated winds (Fig. 1). The state-space modeling of multicorrelated winds used an AR model, and the modeling of unsteady buffeting and self-excited forces was developed using rational function approximations of their frequency dependent characteristics. The proposed approach helps to glean a clear insight into the modeling of wind-induced vibration problems. It begins with a vector of white noise, which is successively transformed to correlated wind fluctuations, aerodynamic forces, and the associated structural motions.

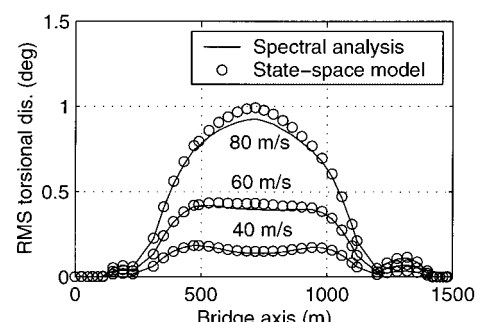
This approach facilitates the use of tools based on linear system theory for the response analysis and structural control design. This procedure allows the time domain simulation of the response to incorporate the frequency dependent unsteady



(a) Lateral displacement



(b) Vertical displacement



(c) Torsional displacement

FIG. 4. Comparison of Buffeting Responses: (a) Lateral Displacement; (b) Vertical Displacement; (c) Torsional Displacement

aerodynamic forces instead of invoking the generally assumed quasi-steady forces. This novel feature enhances the accuracy of the predicted responses. This framework can be utilized in a structural control design by incorporating the wind loading information as a feed-forward link, which has the promise to improve the effectiveness of control. Direct calculations of the covariance matrix of response using the Lyapunov equation offers higher computational efficiency in comparison with conventional spectral analysis approach.

The richness of this analysis framework leads immediately to the next level of analysis, i.e., it can be simply extended to the analysis of bridges/structures with structural and aerodynamic nonlinearities by using a time-variant system model once the nonlinear structural and aerodynamic characteristics of a bridge are established. Both the nonlinear effects and unsteady frequency dependent characteristics of aerodynamic forces can be accurately captured using this scheme. Details will be presented in a future presentation.

Although emphasis in this study was placed on the response of bridges under multicorrelated wind excitation, the proposed approach offers immediate applications to other wind-excited structures as well as systems with frequency dependent parameters, such as those involved in soil-structure and fluid-structure interactions.

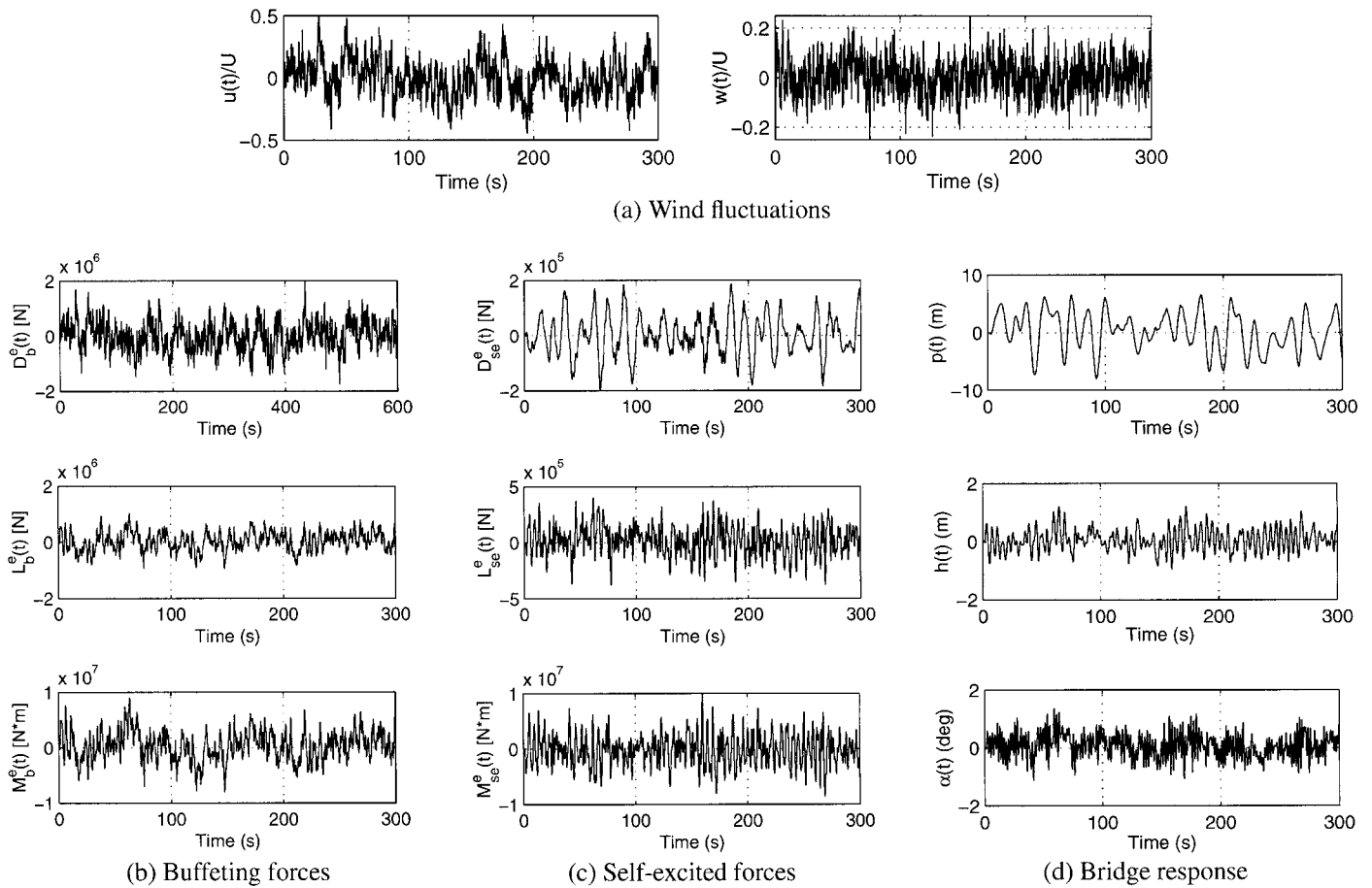


FIG. 5. Simulation of Wind Fluctuations, Buffeting and Self-Excited Forces and Bridge Response ($U = 60$ m/s, at Midpoint of Main Span): (a) Wind Fluctuations; (b) Buffeting Forces; (c) Self-Excited Forces; (d) Bridge Response

APPENDIX I. STATE-SPACE REPRESENTATION OF BUFFETING FORCES F_b^e

The state-space equations for the buffeting forces F_b^e are given as

$$\dot{\mathbf{X}}_b^e = \mathbf{A}_b^e \mathbf{X}_b^e + \mathbf{B}_b^e \mathbf{W}^e \tag{61}$$

$$\mathbf{F}_b^e = \mathbf{C}_b^e \mathbf{X}_b^e + \mathbf{D}_b^e \mathbf{W}^e \tag{62}$$

General Case

Assuming the admittance function χ_r and the joint acceptance J_r ($r = L_{bu}, L_{bw}, D_{bu}, D_{bw}, M_{bu}, M_{bw}$) are unique for each buffeting force components. For each element, totally six admittance functions and six joint acceptance functions need to be expressed in terms of rational functions. Then, the matrices of the state-space model are

$$\mathbf{A}_b^e = \text{diag}[\mathbf{A}_{L_{bu}} \quad \mathbf{A}_{D_{bu}} \quad \mathbf{A}_{M_{bu}} \quad \mathbf{A}_{L_{bw}} \quad \mathbf{A}_{D_{bw}} \quad \mathbf{A}_{M_{bw}}] \tag{63}$$

$$\mathbf{B}_b^e = \begin{bmatrix} \mathbf{B}_{L_{bu}}^T & \mathbf{B}_{D_{bu}}^T & \mathbf{B}_{M_{bu}}^T & \mathbf{0} & \mathbf{0} & \mathbf{0} \\ \mathbf{0} & \mathbf{0} & \mathbf{0} & \mathbf{B}_{L_{bw}}^T & \mathbf{B}_{D_{bw}}^T & \mathbf{B}_{M_{bw}}^T \end{bmatrix}^T \tag{64}$$

$$\mathbf{C}_b^e = (\rho U^2 B l) \begin{bmatrix} C_{L1} C_{L_{bu}} & \mathbf{0} & \mathbf{0} & C_{L2} C_{L_{bw}} & \mathbf{0} & \mathbf{0} \\ \mathbf{0} & C_{D1} C_{D_{bu}} & \mathbf{0} & \mathbf{0} & C_{D2} C_{D_{bw}} & \mathbf{0} \\ \mathbf{0} & \mathbf{0} & 2b C_{M1} C_{M_{bu}} & \mathbf{0} & \mathbf{0} & 2b C_{M2} C_{M_{bw}} \end{bmatrix} \tag{65}$$

$$\mathbf{D}_b^e = (\rho U^2 B l) \begin{bmatrix} C_{L1} D_{L_{bu}} & C_{L2} D_{L_{bw}} \\ C_{D1} D_{D_{bu}} & C_{D2} D_{D_{bw}} \\ 2b C_{M1} D_{M_{bu}} & 2b C_{M2} D_{M_{bw}} \end{bmatrix} \tag{66}$$

$$\mathbf{A}_r = \begin{bmatrix} \mathbf{A}_r^x & \mathbf{0} \\ \mathbf{B}_r^j \mathbf{C}_r^x & \mathbf{A}_r^j \end{bmatrix}; \quad \mathbf{B}_r = \begin{bmatrix} \mathbf{B}_r^x \\ \mathbf{B}_r^j \mathbf{D}_r^x \end{bmatrix} \tag{67a,b}$$

$$\mathbf{C}_r = [\mathbf{D}_r^j \mathbf{C}_r^x \quad \mathbf{C}_r^j]; \quad \mathbf{D}_r = \mathbf{D}_r^j \mathbf{D}_r^x \tag{67c,d}$$

$$\mathbf{A}_r^x = \text{diag}[-d_{r,1}^x U/b \quad \dots \quad -d_{r,m_r^x}^x U/b] \tag{68a}$$

$$\mathbf{B}_r^x = [A_{r,2}^x \quad \dots \quad A_{r,m_r^x+1}^x]^T \tag{68b}$$

$$\mathbf{C}_r^x = [-d_{r,1}^x U/b \quad \dots \quad -d_{r,m_r^x}^x U/b] \tag{69a}$$

$$\mathbf{D}_r^x = A_{r,1}^x + \sum_{j=1}^{m_r^x} A_{r,j+1}^x \tag{69b}$$

$$\mathbf{A}_r^j = \text{diag}[-d_{r,1}^j U/b \quad \dots \quad -d_{r,m_r^j}^j U/b] \tag{70a}$$

$$\mathbf{B}_r^j = [A_{r,2}^j \quad \dots \quad A_{r,m_r^j+1}^j]^T \tag{70b}$$

$$\mathbf{C}_r^j = [-d_{r,1}^j U/b \quad \dots \quad -d_{r,m_r^j}^j U/b] \tag{71a}$$

$$\mathbf{D}_r^j = A_{r,1}^j + \sum_{j=1}^{m_r^j} A_{r,j+1}^j \tag{71b}$$

Special Case

Consider a special case

$$\chi_{Lbu} = \chi_{Lbw} = \chi_{Mbu} = \chi_{Mbw} = \chi_{LM}; \quad \chi_{Dbu} = \chi_{Dbw} = \chi_D \quad (72a,b)$$

$$J_{Lbu} = J_{Dbu} = J_{Mbu} = J_u; \quad J_{Lbw} = J_{Dbw} = J_{Mbw} = J_w \quad (73a,b)$$

In this case, only two admittance functions and two joint acceptance functions need to be expressed in terms of rational functions. The rational function approximations of χ_{LM} , χ_D , J_u , and J_w are given by

$$\chi_r(ik) = A_{r,1}^x + \sum_{j=1}^{m_r^x} \frac{(ik)A_{r,j+1}^x}{ik + d_{r,j}^x} \quad (r = LM, D) \quad (74)$$

$$J_r(ik) = A_{r,1}^j + \sum_{j=1}^{m_r^j} \frac{(ik)A_{r,j+1}^j}{ik + d_{r,j}^j} \quad (r = u, w) \quad (75)$$

and the matrices of the state-space model are given by

$$\mathbf{A}_b^e = \begin{bmatrix} \mathbf{A}_{LM}^x & \mathbf{0} & \mathbf{B}_{LM}^x \mathbf{C}_u^j & & \\ \mathbf{0} & \mathbf{A}_D^x & \mathbf{B}_D^x \mathbf{C}_u^j & & \mathbf{0} \\ \mathbf{0} & \mathbf{0} & \mathbf{A}_u^j & & \\ & & & \mathbf{A}_{LM}^x & \mathbf{0} & \mathbf{B}_{LM}^x \mathbf{C}_w^j \\ \mathbf{0} & & \mathbf{0} & \mathbf{A}_D^x & \mathbf{B}_D^x \mathbf{C}_w^j & \\ & & \mathbf{0} & \mathbf{0} & \mathbf{0} & \mathbf{A}_w^j \end{bmatrix} \quad (76a)$$

$$\mathbf{B}^e = \begin{bmatrix} \mathbf{B}_{LM}^x D_u^j & & & & \\ \mathbf{B}_D^x D_u^j & \mathbf{0} & & & \\ \mathbf{B}_u^j & & & & \\ & & \mathbf{B}_{LM}^x D_w^j & & \\ \mathbf{0} & \mathbf{B}_D^x D_w^j & & & \\ & & & \mathbf{B}_w^j & \end{bmatrix} \quad (76b)$$

$$\mathbf{C}^e = (\rho U^2 B l) \begin{bmatrix} C_{L1} \mathbf{C}_{LM}^x & \mathbf{0} & \mathbf{0} & C_{L2} \mathbf{C}_{LM}^x & \mathbf{0} & \mathbf{0} \\ \mathbf{0} & C_{D1} \mathbf{C}_D^x & \mathbf{0} & \mathbf{0} & C_{D2} \mathbf{C}_D^x & \mathbf{0} \\ BC_{M1} \mathbf{C}_{LM}^x & \mathbf{0} & \mathbf{0} & BC_{M2} \mathbf{C}_{LM}^x & \mathbf{0} & \mathbf{0} \end{bmatrix} \quad (77)$$

$$\mathbf{D}_b^e = (\rho U^2 B l) \begin{bmatrix} C_{L1} D_{LM}^x & C_{L2} D_{LM}^x \\ C_{D1} D_D^x & C_{D2} D_D^x \\ BC_{M1} D_{LM}^x & BC_{M2} D_{LM}^x \end{bmatrix} \quad (78)$$

$$\mathbf{A}_r^x = \text{diag}[-d_{r,1}^x U/b \quad \dots \quad -d_{r,m_r^x}^x U/b] \quad (79a)$$

$$\mathbf{B}_r^x = [A_{r,2}^x \quad \dots \quad A_{r,m_r^x+1}^x]^T \quad (79b)$$

$$\mathbf{C}_r^x = [-d_{r,1}^x U/b \quad \dots \quad -d_{r,m_r^x}^x U/b] \quad (80a)$$

$$D_r^x = A_{r,1}^x + \sum_{j=1}^{m_r^x} A_{r,j+1}^x \quad r = LM, D) \quad (80b)$$

$$\mathbf{A}_r^j = \text{diag}[-d_{r,1}^j U/b \quad \dots \quad -d_{r,m_r^j}^j U/b] \quad (81a)$$

$$\mathbf{B}_r^j = [A_{r,2}^j \quad \dots \quad A_{r,m_r^j+1}^j]^T \quad (81b)$$

$$\mathbf{C}_r^j = [-d_{r,1}^j U/b \quad \dots \quad -d_{r,m_r^j}^j U/b] \quad (82a)$$

$$D_r^j = A_{r,1}^j + \sum_{j=1}^{m_r^j} A_{r,j+1}^j \quad (r = u, w) \quad (82b)$$

ACKNOWLEDGMENTS

The support for this work was provided in part by NSF Grants CMS 9402196, CMS 95-03779, and CMS 00-85019. This support is gratefully acknowledged. The writers are thankful to Dr. Fred Haan, Jr., for his comments on the manuscript.

REFERENCES

- Benfratello, S., and Muscolino, G. (1999). "Filter approach to the stochastic analysis of MDOF wind-excited structures." *Probabilistic Engng. Mech.*, 14, 311–321.
- Boonyapinyo, V., Miyata, T., and Yamada, H. (1999). "Advanced aerodynamic analysis of suspension bridges by state-space approach." *J. Struct. Engng.*, ASCE, 125(12), 1357–1366.
- Bucher, C. G., and Lin, Y. K. (1988). "Stochastic stability of bridges considering coupled modes." *J. Engng. Mech.*, ASCE, 114(12), 2055–2071.
- Chen, X., and Kareem, A. (2000). "On the application of stochastic decomposition in the analysis of wind effects." *Proc., Int. Conf. on Advances in Struct. Dyn.*, Hong Kong, 135–142.
- Chen, X., Matsumoto, M., and Kareem, A. (2000a). "Aerodynamic coupling effects on the flutter and buffeting of bridges." *J. Engng. Mech.*, ASCE, 126(1), 17–26.
- Chen, X., Matsumoto, M., and Kareem, A. (2000b). "Time domain flutter and buffeting response analysis of bridges." *J. Engng. Mech.*, ASCE, 126(1), 7–16.
- Davenport, A. G. (1962). "Buffeting of a suspension bridge by storm winds." *J. Struct. Engng.*, ASCE, 88(3), 233–268.
- Goßmann, E., and Walter, H. B. (1983). "Analysis of multi-correlated wind-excited vibrations of structures using the covariance method." *Engng. Struct.*, 5, 264–272.
- Haan, F. L. (2000). "The effects of turbulence on the aerodynamics of long-span bridges." PhD thesis, University of Notre Dame, Notre Dame, Ind.
- Haan, F. L., Kareem, A., and Szewczyk, A. A. (1999). "Influence of turbulence on the self-excited forces on a rectangular cross section." *Wind Engng. into the 21st Century: Proc., 10th Int. Conf. on Wind Engng.*, Balkema, Rotterdam, The Netherlands, 1665–1672.
- Ianuzzi, A., and Spinelli, P. (1987). "Artificial wind generation and structural response." *J. Struct. Engng.*, ASCE, 113(12), 2382–2398.
- Jain, A., Jones, N. P., and Scanlan, R. H. (1996). "Coupled flutter and buffeting analysis of long-span bridges." *J. Struct. Engng.*, ASCE, 122(7), 716–725.
- Karpel, M. (1982). "Design for active flutter suppression and gust alleviation using state-space aeroelastic modeling." *J. Aircraft*, 19(3), 221–227.
- Kareem, A. (1990). "Measurements of pressure and force fields on building models in simulated atmospheric flows." *J. Wind Engng. and Indust. Aerodyn.*, 36, 589–599.
- Kareem, A. (1997). "Modeling of base-isolated buildings with passive dampers under winds." *J. Wind Engng. and Indust. Aerodyn.*, 72, 323–333.
- Kareem, A., and Mei, G. (1999). "Stochastic decomposition for simulation and modal space reduction in wind induced dynamics of structures." *Application of statistics and probability*, Balkema, Rotterdam, The Netherlands, 757–764.
- Katsuchi, H., Jones, N. P., and Scanlan, R. H. (1999). "Multimode coupled flutter and buffeting analysis of the Akashi-Kaikyo Bridge." *J. Struct. Engng.*, ASCE, 125(1), 60–70.
- Larose, G. L., and Mann, J. (1998). "Gust loading on streamlined bridge decks." *J. Fluids and Struct.*, 12, 511–536.
- Li, Y., and Kareem, A. (1990a). "ARMA system in wind engineering." *Probabilistic Engng. Mech.*, 5(2), 50–59.
- Li, Y., and Kareem, A. (1990b). "Recursive modeling of dynamic systems." *J. Engng. Mech.*, 116(3), 660–679.
- Lin, Y. K., and Yang, J. N. (1983). "Multimode bridge response to wind excitations." *J. Engng. Mech.*, ASCE, 109(2), 586–603.
- Matsumoto, M., and Chen, X. (1996). "Time domain analytical method of buffeting responses for long-span bridges." *Proc., 14th Nat. Symp. on Wind Engng.*, Japan Association for Wind Engineering, 515–520 (in Japanese).
- Matsumoto, M., Chen, X., and Shiraishi, N. (1994). "Buffeting analysis of long-span bridge with aerodynamic coupling." *Proc., 13th Nat. Symp. on Wind Engng.*, Japan Association for Wind Engineering, 227–232 (in Japanese).
- Matsumoto, Y., Fujino, Y., and Kimura, K. (1996). "Wind-induced gust response analysis based on state space formulation." *J. Struct. Mech. and Earthquake Engng.*, 543/1-36, 175–186 (in Japanese).
- Mignolet, M. P., and Spanos, P. D. (1987). "Recursive simulation of stationary multivariate random processes. Part I." *J. Appl. Mech.*, 109, 674–680.
- Ogata, K. (1994). *Discrete-time control systems*, Prentice-Hall, Englewood Cliffs, N.J.
- Roger, K. L. (1977). "Airplane math modeling methods for active control design." *Structural Aspects of Active Controls, AGARD-CP-228*, 4-1–4-11.

- Samaras, E., Shinozuka, M., and Tsurui, A. (1985). "ARMA representation of random processes." *J. Engrg. Mech.*, ASCE, 111(3), 449–461.
- Scanlan, R. H. (1978a). "The action of flexible bridges under wind. I: Flutter theory." *J. Sound and Vibration*, 60(2), 187–199.
- Scanlan, R. H. (1978b). "The action of flexible bridges under wind. II: Buffeting theory." *J. Sound and Vibration*, 60(2), 201–211.
- Scanlan, R. H. (1997). "Amplitude and turbulence effects on bridge flutter derivatives." *J. Struct. Engrg.*, ASCE, 123(2), 232–236.
- Scanlan, R. H., Beliveau, J.-G., and Budlong, K. S. (1974). "Indicial aerodynamic functions for bridge decks." *J. Engrg. Mech. Div.*, ASCE, 100(4), 657–672.
- Soong, T. T., and Grigoriu, M. (1993). *Random vibration of mechanical and structural systems*, Prentice-Hall, Englewood Cliffs, N.J.
- Suhardjo, J., Spencer, B. F., Jr., and Kareem, A. (1992). "Frequency domain optimal control of wind-excited buildings." *J. Engrg. Mech.*, ASCE, 118(12), 2463–2481.
- Wilde, K., Fujino, Y., and Masukawa, J. (1996). "Time domain modeling of bridge deck flutter." *J. Struct. Engrg.*, Tokyo, 13, 93–104.